

# Closed-form expressions for the magnetic field of permanent magnets in three dimensions

V. Ziemann, Uppsala University

February 8, 2022

## Abstract

We derive a closed-form expression of the magnetic field of a finite-size current sheet and use it to calculate the field of permanent magnets, which are modeled through their surface current densities. We illustrate the method by determining the multipoles and the effective length due to fringe fields of a finite-length dipole constructed of magnetic cubes.

## 1 Introduction

Today permanent magnets are widely used in the construction of efficient electrical motors, for example those used in battery-driven automobiles, but also for scientific applications, such as ion traps to store and analyze rare atoms, or for undulators to generate synchrotron radiation, and for multipole magnets to guide and confine charged-particle beams. These magnets do not need to be powered and are therefore very energy efficient, which makes them attractive regarding today's focus on sustainability. In the 1970s Klaus Halbach showed [1] how to design multipole magnets and undulators using paper and pencil only. His approach made use of variables in the complex plane and is essentially limited to two spatial dimensions. In order to analyze three-dimensional features we typically use finite-element codes [2]. In this report, we offer a complementary approach based on solving Biot-Savart's equation for a finite-size rectangular current sheet and modeling the magnets as an assembly of such sheets. In iron-free geometries this allows us to calculate the three components of the magnetic field  $\vec{B}(z)$  at any point in space as the superposition of the contributions from the current-carrying sheets. Since all integrations are done analytically this results in expressions that make calculating the fields very rapid. Moreover, the field values are exact, no approximations due to finite meshes are involved.

A key feature of permanent magnet material is that the relative magnetic permeability  $\mu_r$  is very close to unity, which makes them transparent to other, externally generated fields. As a consequence, the field at a given point  $\vec{z}$  is the

superposition of the fields due to all current sources. And here the second key feature enters; the magnetic field of permanent magnets can be calculated from the equivalent surface current density  $I' = dI/ds = B_r/\mu_0$  that is proportional to the remanent magnetic field  $B_r$  of the permanent magnet material. Here  $\mu_0 = 4\pi \times 10^{-7}$  A/Tm is the permeability of free space. Since  $B_r$  is on the order of one Tesla, the corresponding current densities are enormous.

These observations now guide us through the remainder of this report. We first calculate the field of a straight current-carrying filament, followed by spreading the filament laterally to obtain a current sheet and calculating the field it generates. In the subsequent section we briefly introduce software, based on MATLAB, to assemble magnets that are composed of these sheets and calculate their fields. We then use the software to illustrate the field of a single sheet, a magnet cube assembled of four sheets, and a dipole magnet, made of four cubes, whose field quality and fringe fields we analyze. Finally, we consider solenoid magnets which help us to validate the calculations and the software.

## 2 Field of a filament

The magnetic field at point  $\vec{r}_2$  due to a filament that carries a current  $I$ , starts at position  $\vec{r}_a$ , and ends at  $\vec{r}_b$  is given by Biot-Savart's law

$$\vec{B}(\vec{r}_2) = \frac{\mu_0 I}{4\pi} \int \frac{d\vec{r}_1 \times (\vec{r}_2 - \vec{r}_1)}{|\vec{r}_2 - \vec{r}_1|^3} = \frac{\mu_0 I}{4\pi} \int_0^1 \frac{[\vec{r}_b - \vec{r}_a] \times [\vec{r}_2 - t\vec{r}_b - (1-t)\vec{r}_a]}{|\vec{r}_2 - t\vec{r}_b - (1-t)\vec{r}_a|^3} dt, \quad (1)$$

where we parameterize a point on the filament  $\vec{r}_1$  by  $\vec{r}_1 = (1-t)\vec{r}_a + t\vec{r}_b$  with  $0 < t < 1$ . First we simplify the numerator in the last equality and find

$$(\vec{r}_b - \vec{r}_a) \times (\vec{r}_2 - t\vec{r}_b - (1-t)\vec{r}_a) = (\vec{r}_b - \vec{r}_a) \times (\vec{r}_2 - \vec{r}_a) \quad (2)$$

whereas for the denominator we obtain

$$\begin{aligned} |\vec{r}_2 - t\vec{r}_b - (1-t)\vec{r}_a|^2 &= (\vec{r}_2 - t\vec{r}_b - (1-t)\vec{r}_a) \cdot (\vec{r}_2 - t\vec{r}_b - (1-t)\vec{r}_a) \\ &= (\vec{r}_2 - \vec{r}_a)^2 - 2t(\vec{r}_2 - \vec{r}_a) \cdot (\vec{r}_b - \vec{r}_a) + t^2(\vec{r}_b - \vec{r}_a)^2 \\ &= A - 2Bt + Ct^2 \end{aligned} \quad (3)$$

with

$$A = (\vec{r}_2 - \vec{r}_a)^2, \quad B = (\vec{r}_2 - \vec{r}_a) \cdot (\vec{r}_b - \vec{r}_a), \quad \text{and} \quad C = (\vec{r}_b - \vec{r}_a)^2. \quad (4)$$

Note that these parameters have simple geometric interpretations:  $A$  describes the squared distance  $d_P$  between the observation point  $P$  at  $\vec{r}_2$  and the starting point of the filament  $\vec{r}_a$ . The variable  $B$  is the product of  $d_P$ , the length  $L$  of the filament, and the cosine of the enclosed angle, whereas  $C$  is the length of the

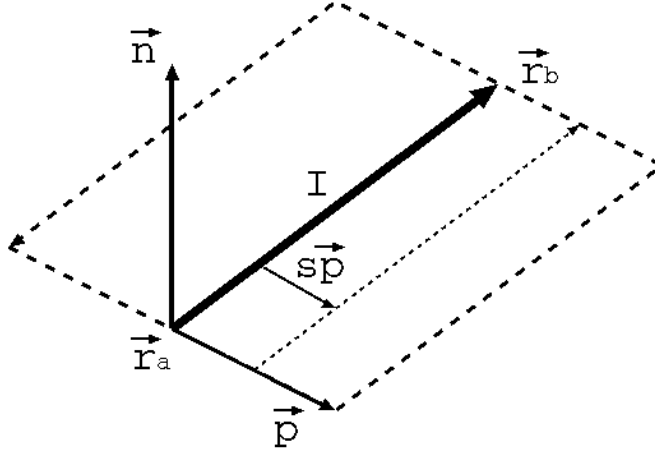


Figure 1: Current sheet.

filament squared. Inserting these expressions into the equation for the magnetic field  $\vec{B}$  we get

$$\vec{B}(\vec{r}_2) = \frac{\mu_0 I}{4\pi} (\vec{r}_b - \vec{r}_a) \times (\vec{r}_2 - \vec{r}_a) \int_0^1 \frac{dt}{(A - 2Bt + Ct^2)^{3/2}}. \quad (5)$$

This integral can be found in integral tables [3] and is given by

$$\int \frac{dt}{(A - 2Bt + Ct^2)^{3/2}} = \frac{Ct - B}{(AC - B^2)\sqrt{A - 2Bt + Ct^2}} \quad (6)$$

such that we write  $\vec{B}(\vec{r}_2)$  as

$$\vec{B}(\vec{r}_2) = \frac{\mu_0 I}{4\pi} \frac{(\vec{r}_b - \vec{r}_a) \times (\vec{r}_2 - \vec{r}_a)}{AC - B^2} \left[ \frac{C - B}{\sqrt{A - 2B + C}} + \frac{B}{\sqrt{A}} \right] \quad (7)$$

where  $A, B$  and  $C$  are given in Equation 4. Equation 7 is already quite useful to determine the fields of systems containing a finite number of current-carrying wires. We previously used it to design earth-field compensation coils [4].

### 3 Field of a finite current sheet

In order to calculate the field of a sheet, we first consider the field that is generated by a filament that is laterally displaced by the vector

$$\vec{p} = \alpha(\vec{r}_b - \vec{r}_a) \times \vec{n}, \quad (8)$$

where  $\vec{n}$  is the vector normal to the sheet and  $\alpha$  is the aspect ratio of the sheet, such that  $w = \alpha|\vec{r}_b - \vec{r}_a| = \alpha\sqrt{C}$  is the width of the sheet. The construction is

illustrated in Figure 1. Note that  $\vec{p}$  is perpendicular to the filament; the scalar product of  $\vec{r}_b - \vec{r}_a$  and  $\vec{p}$  is zero. This construction permits us to parameterize the parallel-displaced filament by its end points  $\vec{r}_a + s\vec{p}$  and  $\vec{r}_b + s\vec{p}$ , where  $1/2 \leq s \leq 1/2$  describes by how far the filament is displaced, as shown in Figure 1 by the thin dotted line that is parallel to  $\vec{r}_b - \vec{r}_a$ . The field from the displaced filament is then given by replacing the parameters  $A, B$  and  $C$  by their  $s$ -dependent counterparts given by

$$\begin{aligned} A(s) &= (\vec{r}_2 - \vec{r}_a - s\vec{p})^2 \\ B(s) &= (\vec{r}_2 - \vec{r}_a - s\vec{p}) \cdot (\vec{r}_b - \vec{r}_a) \\ C(s) &= (\vec{r}_b + s\vec{p} - \vec{r}_a - s\vec{p})^2 = C . \end{aligned} \quad (9)$$

Moreover, the cross-product before the integral becomes  $(\vec{r}_b - \vec{r}_a) \times (\vec{r}_2 - \vec{r}_a - s\vec{p})$ . We now “spread out” the current  $I = I'w$  evenly across the width  $w = \alpha\sqrt{C}$  of the sheet with constant current density  $I'$  and sum up the contributions of all displaced filaments, which corresponds to integrating over  $s$ . We also note that the current density  $I'$  is related to the remanent magnetic field  $B_r$  through  $\mu I' = B_r$ . Combining these concepts we find that the the field at point  $\vec{r}_2$  is given by the following integral

$$\begin{aligned} \vec{B}(\vec{r}_2) &= \frac{B_r \alpha \sqrt{C}}{4\pi} \int_{-1/2}^{1/2} \frac{(\vec{r}_b - \vec{r}_a) \times (\vec{r}_2 - \vec{r}_a - s\vec{p})}{A(s)C - B(s)^2} \\ &\quad \times \left[ \frac{C - B(s)}{\sqrt{A(s) - 2B(s) + C}} + \frac{B(s)}{\sqrt{A(s)}} \right] ds \end{aligned} \quad (10)$$

where  $A(s)$  and  $B(s)$  are at most quadratic functions of  $s$ . The evaluation of the integral, which is rather lengthy and therefore deferred to Appendix A, leads to

$$\begin{aligned} \vec{B}(\vec{r}_2) &= \frac{B_r \alpha C}{4\pi} [(C - B)J_1 + BJ_3] (\vec{r}_b - \vec{r}_a) \times (\vec{r}_2 - \vec{r}_a) \\ &\quad + \frac{B_r \alpha C^2}{4\pi} [(C - B)J_2 + BJ_4] \vec{n} , \end{aligned} \quad (11)$$

where  $J_1$  to  $J_4$  are defined in Appendix A in Equations 22 to 24. We point out that  $\alpha C$  is the area of the sheet, such that  $B_r \alpha C$  describes the integrated “strength” of the sheet to excited magnetic fields.

## 4 Software implementation

Equation 11 describes the magnetic field vector  $\vec{B}(\vec{r}_2)$  that is caused by one sheet that is characterized by  $\vec{r}_a, \vec{r}_b, \vec{n}, \alpha, B_r$  in a coordinate-free way and only requires function evaluations; no integrations are necessary which makes the calculation

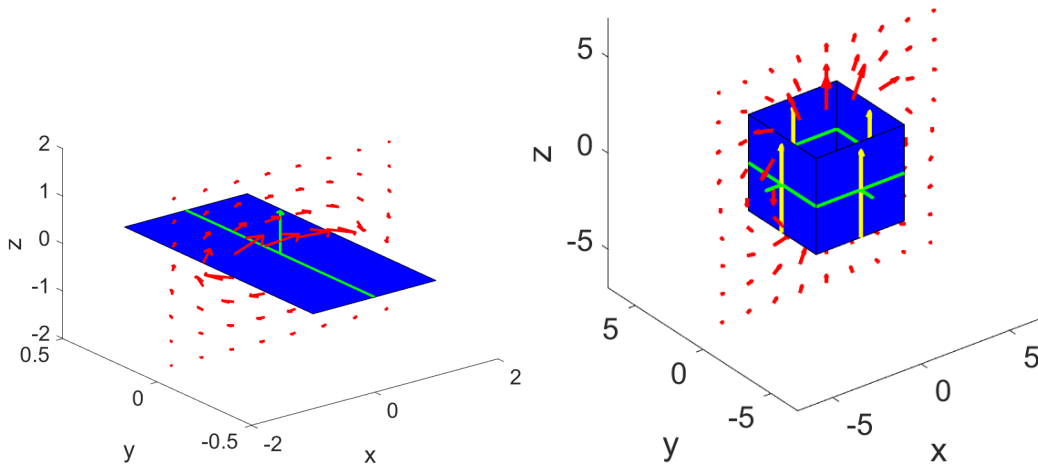


Figure 2: Field pattern of a current sheet (left) and a four sheets assembled to generate the field of a permanent magnet cube (right).

of  $\vec{B}(\vec{r}_2)$  very fast. In order to calculate the field at a given point  $\vec{r}_2$  due to several sheets we only have to sum over the contributions from each of the sheets.

We therefore represent each sheet by a one-dimensional array that contains the three spatial components of  $\vec{r}_a, \vec{r}_b, \vec{n}$  as well as  $\alpha$  and  $B_r$  for that sheet; thus there are eleven numbers to store for each sheet. The entire geometry is then given as a collection of, say  $M$ , such sheets that is stored in an array of dimension  $M \times 11$ .

In order to place the sheets within the geometry, we prepare functions to translate sheets by a vector  $\vec{a}$ ; the function simply adds  $\vec{a}$  to  $\vec{r}_a$  and  $\vec{r}_b$  in the array with the sheets. Likewise, three functions to rotate a sheet by an angle  $\theta$  around each of the three axes, just multiply  $\vec{r}_a, \vec{r}_b$ , and  $\vec{n}$  in a sheet by the appropriate rotation matrix. Using these functions, it is easy to create any geometry, very similar to the way that three-dimensional modeling software composes complex geometries from geometric primitives, often triangles, but also from cubes or spheres.

Finally functions to calculate the field at a point or along a path just loop over the sheets and add their contributions. We implemented these functions in MATLAB, briefly explain the functions in Appendix B, and illustrate their use with a number of simple examples in the next section.

## 5 Examples

As a first example we consider the field of a single sheet, which is shown on the left-hand image in Figure 2. The sheet is shown as the blue rectangle and the current as the green line stretching in the center of the sheet. The vertical green

arrow indicates the normal vector  $\vec{n}$  of the sheet. We observe that the magnetic field vector  $\vec{B}$  curls around the sheet, perpendicular to the current's direction, pointing to the right above and to the left below the sheet. Making the sheets very narrow causes the field to approach a circular form, just as expected from Ampere's law.

In the next step we assemble four quadratic current sheets to represent a permanent magnet cube, which is shown on the right-hand image in Figure 2. We see that the current, again shown as a green line, flows around the surface of the cube. We use the convention that the normal vectors, again shown as green arrows, point towards the outside of the magnet. The easy axis of the magnet is indicated by the yellow arrow on the sheets, that is oriented perpendicular to the current flow and points upwards. The magnetic field created by the four sheets representing the permanent magnet cube is illustrated by the red arrows. We observe that the field points upwards at the top of the cube, then turns over such that it points down on the outside of the cube, then turns over again to point upwards below the cube. We point out that the four current sheets form a square solenoid and the field therefore corresponds to that geometry.

We reach the next level of complexity by assembling eight 5 mm-cubes with  $B_r = 1.47$  T to form an approximation of a Halbach dipole, discussed in Appendix A.3 in [5]. The top left image in Figure 3 shows the view onto the assembly from the top. The easy axis of the magnets, shown by the yellow arrows, rotates twice when moving from one magnet to the next; in every fourth of the eight magnets it points in the same direction. In the center of the assembly, the magnetic field points upwards, as is expected for a dipole. The plot on the top right shows the vertical field component  $B_y$  along the black dotted line shown on the left-hand image. We observe that the field is on the order of 0.35 T and has a small dip in the center. The image on the left-hand side in the middle row shows a perspective view of the same geometry which makes the three-dimensional character obvious. The vertical red line in the center of the assembly indicates the direction of the  $z$ -axis and the plot on its right shows  $B_y$  along this direction, but extending over  $\pm 20$  mm. We see that the peak field of about 0.35 T appears in the center of the magnet, but the fringe field extends significantly outside the magnet, which only has a height of  $\pm 2.5$  mm.

We determine the multipolarity of the assembly at the radius  $r$  shown by the cyan circle on the top-left image. A tangent to the circle, illustrated by the cyan straight line, is also shown. In order to determine the multipoles we calculate the scalar product of the tangent vector with the magnetic field at every point on the circle. This yields the tangential field component  $B_t$  which we display in the top panel of the image at the bottom left plot as a function of the azimuthal angle  $\phi$ . The multipolarity, shown on the middle panel then follows from a Fourier-transformation, as discussed in Appendix C. We find that mainly the dipole component with multipolarity  $m = 1$  is present and that its amplitude is  $B_{max} = 0.353$  T. Moreover, from the real and imaginary part of the transform,

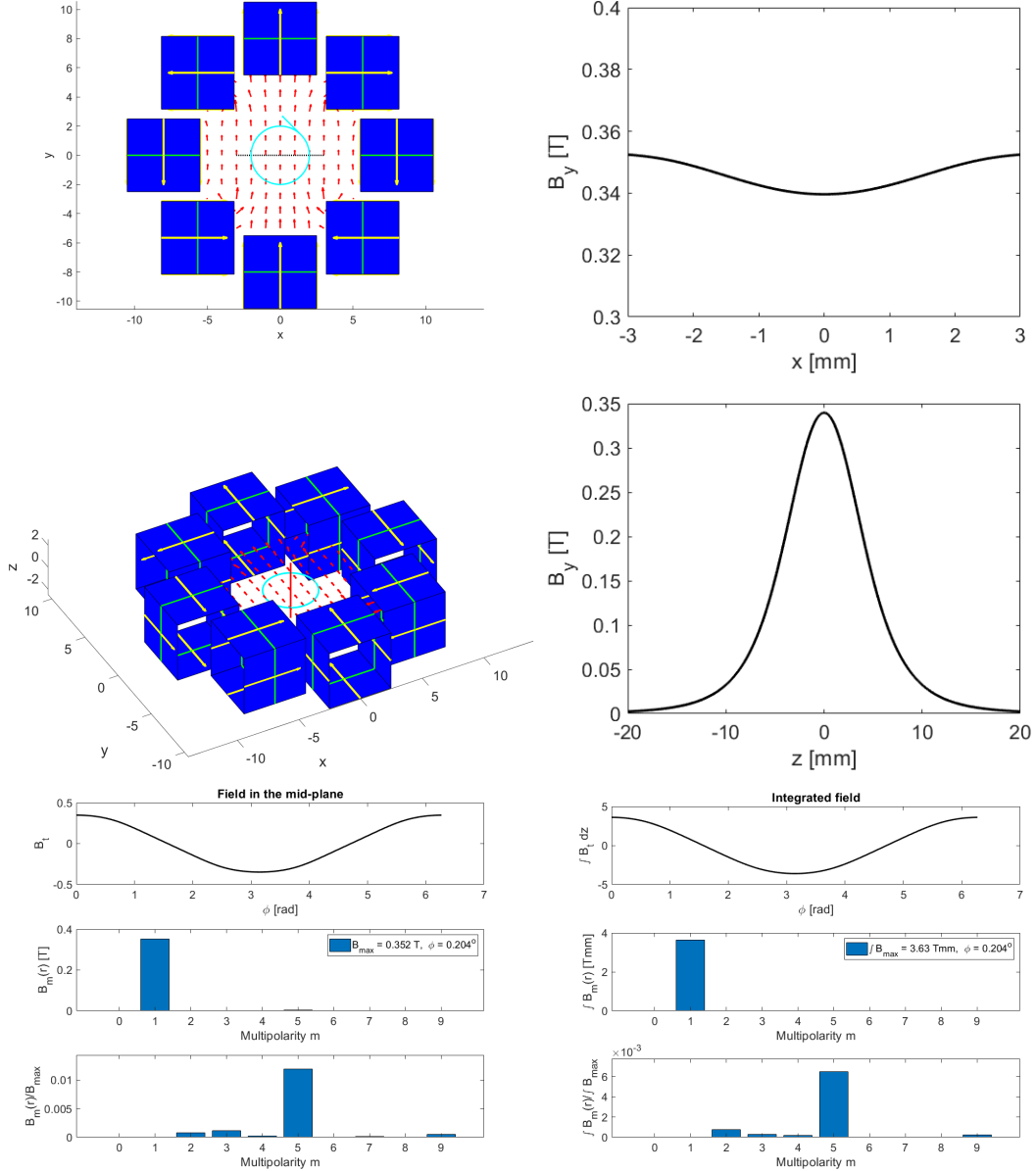


Figure 3: The geometry of a permanent magnet solenoid (top left) and the vertical field in the midplane in the  $x$ -direction (top right). A 3D rendition of the magnet (middle left) and the field along the  $z$ -axis (middle right). The bottom left shows the field along the circle shown in cyan and the multipole coefficients (absolute and relative) in the midplane. The bottom right shows the corresponding integrated values.

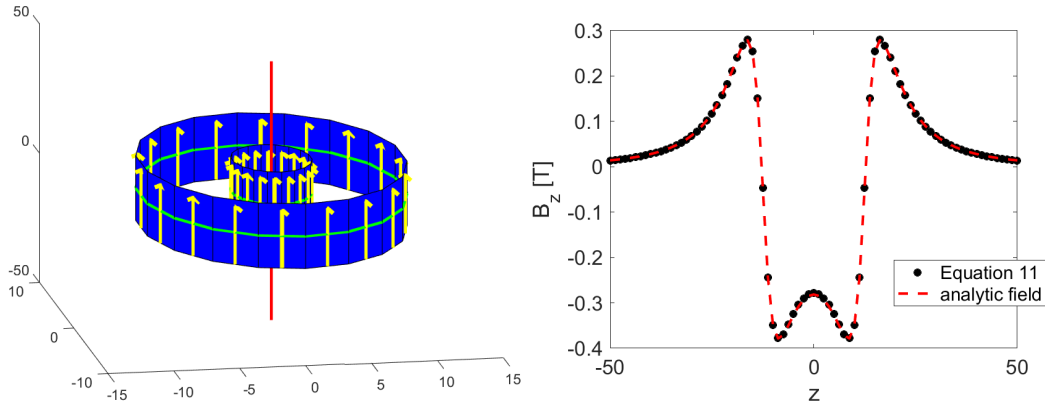


Figure 4: The geometry of a permanent magnet solenoid (left) and the field on axis (right).

we determine the roll angle of the magnet, which here turns out to be close to zero. On the bottom panel we show the amplitudes of the higher multipoles, normalized to  $B_{max}$ . We find the decapole component ( $m = 5$ ) with a relative amplitude on the order of a percent to give the dominant contribution. Finally, we calculate the integral of  $B_t$  along a line in the range  $z = \pm 20$  mm with  $x$  and  $y$ -positions determined by the cyan circle and display it on the upper panel in the image on the bottom-right of Figure 3. Again, mostly the dipole component with  $m = 1$  is present. Moreover the field integral turns out to be 3.63 Tmm, which allows us to determine the effective length of the magnet to be about 10.3 mm, a value that significantly exceeds the physical length of the magnet, which is only 5 mm. Again the decapole component with a relative magnitude of about  $6 \times 10^{-3}$  gives the dominant contribution to the integrated field.

As last example we consider an axial permanent magnet solenoid with  $B_r = 1.47$  T, inner radius 3 mm, and outer radius 10 mm. It is modeled by circular currents flowing in one direction at the inner radius and in the opposite direction at the outer radius. The left-hand image in Figure 4 shows the assembly, here the circular magnet is approximated by a hollow polygon with 18 sides. The field along the central axis of two long concentric circular solenoids is known analytically [6]. We therefore compare it to our numerical solution, based on Equation 11, and show both on the right-hand plot in Figure 4. We observe that the agreement is very good.

## 6 Conclusions

We determined an analytic expression for the magnetic field generated by a rectangular current sheet and used it to model permanent magnets in iron-free ge-

ometries. We illustrated the method by calculating the fields of simple geometries such as a single sheet, cubes, and solenoids assembled from multiple sheets.

We expect this algorithm to be useful for rapid prototyping of three-dimensional permanent-magnet structures. It is rather fast because all integrations are done analytically and only fields at the points of interest need to be calculated. This is in contrast to finite-element methods. They first need to determine the fields on a grid in the whole geometry and then interpolate the fields to the points of interest. On the other hand is the present method limited to iron-free geometries and to magnets that can be modeled with rectangular current sheets.

Discussions with Roger Ruber are gratefully acknowledged. In part, funding is provided through the project *Disseminating technology for cold magnets to provide access to a wider international market* that is supported by the European Regional Development Fund (ERDF) and Region Kronoberg.

## References

- [1] K. Halbach, *Design of permanent multipole magnets with oriented rare earth cobalt magnets*, Nuclear Instruments and Methods 169 (1980) 1.
- [2] Finite-element codes, for example, COMSOL <https://www.comsol.com>.
- [3] I. Gradstein, I. Ryzhik, *Tables of series, products, and integrals*, Verlag Harri Deutsch, Thun, 1981.
- [4] V. Ziemann, R. Wedberg, T. Peterson, A. Wiren, *Retro-Fitting Earth-Field Compensation Coils to the Vertical Cryostat GERSEMI in FREIA*, Instruments 2020, 4(1), 8.
- [5] V. Ziemann, *Hands-On Accelerator Physics Using MATLAB*, CRC Press, Boca Raton, 2019.
- [6] Q. Peng, S. McMurry, J. Coey, *Axial magnetic field produced by axially and radially magnetized permanent rings*, Journal of Magnetism and Magnetic Materials 268 (2004) 165.

## A The integral

In this appendix we evaluate the integral, given in Equation 10. First we consider the cross product before the integral

$$\begin{aligned}
 (\vec{r}_b - \vec{r}_a) \times (\vec{r}_2 - \vec{r}_a - s\vec{p}) & \\
 &= (\vec{r}_b - \vec{r}_a) \times (\vec{r}_2 - \vec{r}_a) - \alpha s (\vec{r}_b - \vec{r}_a) \times [(\vec{r}_b - \vec{r}_a) \times \vec{n}] \\
 &= (\vec{r}_b - \vec{r}_a) \times (\vec{r}_2 - \vec{r}_a) + s\alpha C \vec{n}
 \end{aligned} \tag{12}$$

where we used the identity  $\vec{a} \times [\vec{b} \times \vec{c}] = \vec{b}(\vec{a} \cdot \vec{c}) - \vec{c}(\vec{a} \cdot \vec{b})$  to evaluate the double cross product in the second line. Next, we calculate

$$A(s) = (\vec{r}_2 - \vec{r}_a)^2 - 2s(\vec{r}_2 - \vec{r}_a) \cdot \vec{p} + s^2 \vec{p}^2 = A - 2Ds + s^2 \vec{p}^2 \quad (13)$$

where we introduce  $D = (\vec{r}_2 - \vec{r}_a) \cdot \vec{p}$ . For  $\vec{p}^2$  in the last term we find

$$\begin{aligned} \vec{p}^2 &= \alpha^2 [(\vec{r}_b - \vec{r}_a) \times \vec{n}] \cdot [(\vec{r}_b - \vec{r}_a) \times \vec{n}] \\ &= \alpha^2 [(\vec{r}_b - \vec{r}_a)^2 \vec{n}^2 - ((\vec{r}_b - \vec{r}_a) \cdot \vec{n})^2] = \alpha^2 C, \end{aligned} \quad (14)$$

which allows us to write

$$A(s) = A - 2Ds + \alpha^2 C s^2 \quad (15)$$

as a second-order polynomial in the variable  $s$ . For  $B(s)$  we arrive at

$$\begin{aligned} B(s) &= (\vec{r}_2 - \vec{r}_a - s\vec{p}) \cdot (\vec{r}_b - \vec{r}_a) \\ &= B - s\alpha [(\vec{r}_b - \vec{r}_a) \times \vec{n}] \cdot (\vec{r}_b - \vec{r}_a) = B, \end{aligned} \quad (16)$$

which is constant. Inserting these parameters into Equation 10 leads to

$$\begin{aligned} \vec{B}(\vec{r}_2) &= \frac{\mu_0 I' \alpha \sqrt{C}}{4\pi} \int_{-1/2}^{1/2} ds \frac{(\vec{r}_b - \vec{r}_a) \times (\vec{r}_2 - \vec{r}_a) + \alpha s C \vec{n}}{AC - B^2 + C^2 - 2sCD + \alpha^2 C^2 s} \\ &\quad \left[ \frac{\sqrt{C}(C - B)}{\sqrt{AC - 2BC + C^2 - 2sCD + \alpha^2 C^2 s^2}} + \frac{\sqrt{C}(B)}{\sqrt{AC - 2sCD + \alpha^2 C^2 s^2}} \right]. \end{aligned} \quad (17)$$

Close inspection of the integrand shows that the second-order polynomial in the denominator of the first line only differs by a constant term from the polynomials under the roots in the second line. Introducing the abbreviations

$$R_1 = a_1 + b_1 s + c_1 s^2 \quad \text{with} \quad a_1 = AC - 2BC + C^2, \quad b_1 = -2CD, \quad c_1 = \alpha^2 C^2 \quad (18)$$

and

$$R_2 = a_2 + b_2 s + c_2 s^2 \quad \text{with} \quad a_2 = AC, \quad b_2 = -2CD = b_1, \quad c_2 = \alpha^2 C^2 = c_1 \quad (19)$$

we can write

$$\begin{aligned} \vec{B}(\vec{r}_2) &= \frac{\mu_0 I' \alpha C}{4\pi} \int_{-1/2}^{1/2} ds \left[ \frac{(\vec{r}_b - \vec{r}_a) \times (\vec{r}_2 - \vec{r}_a) + \alpha s C \vec{n}}{p_1 + R_1} \frac{C - B}{\sqrt{R_1}} \right. \\ &\quad \left. + \frac{(\vec{r}_b - \vec{r}_a) \times (\vec{r}_2 - \vec{r}_a) + \alpha s C \vec{n}}{p_2 + R_2} \frac{B}{\sqrt{R_2}} \right] \\ &= \frac{\mu_0 I' \alpha C}{4\pi} \left[ (\vec{r}_b - \vec{r}_a) \times (\vec{r}_2 - \vec{r}_a) (C - B) \int_{-1/2}^{1/2} \frac{ds}{(p_1 + R_1) \sqrt{R_1}} \right. \\ &\quad + \vec{n} \alpha C (C - B) \int_{-1/2}^{1/2} \frac{s ds}{(p_1 + R_1) \sqrt{R_1}} \\ &\quad + (\vec{r}_b - \vec{r}_a) \times (\vec{r}_2 - \vec{r}_a) B \int_{-1/2}^{1/2} \frac{ds}{(p_2 + R_2) \sqrt{R_2}} \\ &\quad \left. + \vec{n} \alpha C B \int_{-1/2}^{1/2} \frac{s ds}{(p_2 + R_2) \sqrt{R_2}} \right] \quad (20) \end{aligned}$$

with  $p_1 = -(B - C)^2$  and  $p_2 = -B^2$ . We denote the integrals by

$$\begin{aligned} J_1 &= \int_{-1/2}^{1/2} \frac{ds}{(p_1 + R_1)\sqrt{R_1}}, & J_2 &= \int_{-1/2}^{1/2} \frac{s ds}{(p_1 + R_1)\sqrt{R_1}}, \\ J_3 &= \int_{-1/2}^{1/2} \frac{ds}{(p_2 + R_2)\sqrt{R_2}}, & J_4 &= \int_{-1/2}^{1/2} \frac{s ds}{(p_2 + R_2)\sqrt{R_2}}. \end{aligned} \quad (21)$$

We note that  $J_3$  and  $J_4$  resemble  $J_1$  and  $J_2$ , only the constant parameters  $a_i, b_i, c_i$ , and  $p_i$  for  $i = 1, 2$  differ. We therefore only consider  $J_1$  and  $J_2$  in the following. As a matter of fact, closed expressions for these integrals are given as number 2.284 in [3]. In particular  $J_1$  and  $J_2$  can be determined from

$$UJ_2 + VJ_1 = \int \frac{Us + V}{(p_1 + R_1)\sqrt{R_1}} ds = \frac{U}{c_1} I_1(s) - \frac{2Vc_1 - Ub_1}{\sqrt{c_1^2 p_1 [b_1^2 - 4(a_1 + p_1)c_1]}} I_2(s) \quad (22)$$

with  $I_1(s)$  given by [3]

$$I_1(s) = \begin{cases} \frac{1}{\sqrt{p_1}} \arctan\left(\sqrt{\frac{R_1}{p_1}}\right) & \text{for } p_1 > 0 \\ \frac{1}{2\sqrt{-p_1}} \ln\left(\frac{\sqrt{-p_1} - \sqrt{R_1}}{\sqrt{-p_1} + \sqrt{R_1}}\right) & \text{for } p_1 < 0. \end{cases} \quad (23)$$

With  $d_1 = b_1^2 - 4(a_1 + p_1)c_1$  the second contribution  $I_2(s)$  is given by [3]

$$I_2(s) = \begin{cases} -\arctan\left(\sqrt{\frac{p_1}{d_1}}\right) \frac{b_1 + 2c_1 s}{\sqrt{R_1}} & \text{for } p_1 d_1 > 0 \\ \frac{1}{2i} \ln\left(\frac{\sqrt{-d_1}\sqrt{R_1} + \sqrt{p_1}(b_1 + 2c_1 s)}{\sqrt{-d_1}\sqrt{R_1} - \sqrt{p_1}(b_1 + 2c_1 s)}\right) & \text{for } p_1 d_1 < 0 \text{ and } p_1 > 0 \\ \frac{1}{2i} \ln\left(\frac{\sqrt{d_1}\sqrt{R_1} + \sqrt{-p_1}(b_1 + 2c_1 s)}{\sqrt{d_1}\sqrt{R_1} - \sqrt{-p_1}(b_1 + 2c_1 s)}\right) & \text{for } p_1 d_1 < 0 \text{ and } p_1 < 0 \end{cases} \quad (24)$$

where  $R_1$  is a function of  $s$ , given in Equation 18. We point out that the sign of  $I_2(s)$  in Equation 22 is reversed with respect to [3] to make the numerically evaluated integral consistent with the value given in Equation 24. Inserting  $J_1$  through  $J_4$  in Equation 20 and reordering terms then leads to the result stated in Equation 11 in the main body of this report.

## B MATLAB functions

The following MATLAB functions implement the functionality described in Section 4 and are used to generate the plots shown in the main body of this report. Note that `sheets` is a  $M \times 11$  array that describes  $M$  sheets.

- `B=Bsheets(sheets,r2)`: returns  $\vec{B}(\vec{r}_2)$  for the sheets defined by the input argument.
- `sheets=make_cubez(a,alpha,Br)`: returns the four sheets for a square block with width  $a$  and height  $\alpha a$  with the easy axis pointing in the  $z$ -direction.

- `sheets=make_brick(a,b,c,Br)`: returns the four sheets for a rectangular block with sizes  $a, b$ , and  $c$  in the  $x, y$ , and  $z$  direction, respectively. The easy axis points in the  $z$ -direction.
- `sheets=make_polygon(n,r,h,Br)`: returns the  $n$  sheets for a polygon with  $n$  sides, where  $r$  specifies the distance from the center to the corners and  $h$  is the height in the  $z$  direction. The easy axis also points in the  $z$ -direction.
- `sheets=make_polygon_hollow(n,ri,ro,h,Br)`: returns the  $2n$  sheets for a hollow polygon with  $n$  sides, where  $r_i$  specifies the distance from the center to the corners of the inner polygon and  $r_o$  to the outer polygon;  $h$  is the height in the  $z$  direction. The easy axis also points in the  $z$ -direction. This function creates “solenoidal” permanent magnets with single call.
- `sheets=sheets_translate(sheets,a)`: returns the sheets provided as input after adding a vector  $\vec{a}$  to  $\vec{r}_a$  and  $\vec{r}_b$  of the sheets.
- `sheets=sheets_rotate_x(sheets,theta)`: returns the sheets provided as input after the corresponding vectors  $\vec{r}_a, \vec{r}_b$ , and  $\vec{n}$  of the sheets are rotated by the angle  $\theta$ . There are corresponding functions for rotations around the  $y$  and  $z$ -axis.
- `draw_sheet(sheet)`: draws one sheet as a blue surface and adds a green line to indicate the direction of the current flow. A yellow arrow indicates the easy axis.
- `B=field_along_line(sheets,line)`: returns an array of  $\vec{B}(\vec{r}_2)$  at the sequence of points  $\vec{r}_2$  provided in the array `line`.

The use of these functions is best illustrated in the code to prepare a Halbach multipole. The code below first prepares a 5 mm cube and the rotates it such that the easy axis points in the vertical direction. After defining the number of cubes and the multipolarity we loop over the cubes. Inside the loop we first rotate the cube as needed to generate the desired multipolarity  $m$ , then translate it radially along the  $x$  axis by 8 mm before rotating into place a second time. Last, we add the sheets of the currently handled cube to the `sheets` which, after the loop completes, contains all the sheets that define the multipole.

```

cube=make_cubez(5,1,Br);
cubey=sheets_rotate_x(cube,-90);
MM=8; % number of cubes
m=1; % multipolarity (m=1: dipole, 2: quadrupole)
for k=0:MM-1
    tmp=sheets_rotate_z(cubey,-k*m*360/MM);
    tmp=sheets_translate(tmp,[8;0;0]);

```

```

tmp=sheets_rotate_z(tmp,-k*360/MM);
if k==0
    sheets=tmp;
else
    sheets=[sheets;tmp];
end
end

```

## C Determining the multipolarity

On magnet test benches the multipolarity of magnets is often determined from the voltage that is induced in a coil that rotates inside the magnet. In a dipole the polarity changes once per revolution and the voltage shows a spectral component at the revolution frequency. In a quadrupole, the polarity changes twice per revolution and the spectrum shows a peak at the second revolution harmonic, whose amplitude is proportional to the quadrupole gradient.

Here, we use a simplified version of this procedure and calculate the projection of the magnetic field onto a (normalized) vector that is tangent to a circle with radius  $r$  inside the magnet. This is illustrated by the cyan circle and tangent vector visible on the top-left image in Figure 3. In much the same way as on a measurement bench, the number of polarity changes when traveling around the circle is related to the multipolarity  $m$  of the magnet. The amplitude  $\hat{B}$  of the Fourier harmonic directly gives the magnetic field harmonic on the circle. For example, in a quadrupole,  $\hat{B}$  is related to the gradient  $g$  by  $g = \hat{B}/r$ .

Moreover, if we denote the real and imaginary part of the largest Fourier harmonic by  $a_m + ib_m$ , the roll angle  $\hat{\phi}$  of the magnet around the  $z$ -axis (pointing upwards on the top-left image in Figure 3) is given by  $\hat{\phi} = (1/m) \arctan(b_m/a_m)$ . In the legend of the images in the bottom row this value is also reported. It is, however, very small, because the magnet was not rotated.

If we use the field on the cyan circle, we measure the harmonic at a given  $z$ -position, similar to what a short rotating coil would do. If, on the other hand, we integrate the field along a line extending in the  $z$ -direction and perpendicular to positions on the circle, we determine the harmonics of the integrated field, similar to what a long coil would do. This information is reported on the bottom left image in Figure 3.